# Inhibition of Acetylcholinesterase by Physostigmine Analogs: Conformational Mobility of Cysteine Loop Due to the Steric Effect of the Alkyl Chain

*Enrico Gavuzzo*[1] *and Massimo Pomponi*[2]

[1]Ist. di Strutturistica Chimica, CNR Montelibretti

[2]Ist. di Chimica, Facoltà di Medicina, UCSC, Rome, Italy; E-mail: *m.pomponi@rm.unicatt.it*

*Received 31 July 2001; revised 27 February 2002; accepted 12 March 2002*

**ABSTRACT: The effect of a series of physostigmine analogs on acetylcholinesterase activity was investigated. The second-order rate constant $k_{on}$ of the enzyme–inhibitor complex correlates with the conformational positioning of aromatic residues, especially Trp84, in the transition state complex. The van der Waals interactions are an important structural element of this conformational change. A transient mobility of the cysteine loop (Cys67–Cys94) was confined only to the presence of a significant steric effect. Even with this limitation, however, the steric effect seems to be an appropriate model for future tests on the "back door" hypothesis involving facilitated opening for faster product clearance.** © 2002 Wiley Periodicals, Inc. J Biochem Mol Toxicol 16:64–69, 2002; Published online in Wiley Interscience (www.interscience.wiley.com). DOI 10.1002/jbt.10026

KEYWORDS: **Inhibition of AChE; Cysteine Loop (Cys67–Cys94); Steric Effects**

## INTRODUCTION

Acetylcholinesterase (AChE, EC 3.1.1.7) inhibitors donepezil, tacrine, and physostigmine are the only FDA-approved primary treatment for patients with mild to moderately severe Alzheimer's disease [1]. However, notwithstanding the abundance of data collected on the extraordinary catalytic efficiency of AChE, comprehensive characterization of AChE structure–function relationships has only lately begun to emerge. However, the X-ray 3-D structure of *Torpedo californica* AChE (*Tc*AChE) [2] revealed that its active site is deeply buried within the molecule, in a long and narrow gorge lined with aromatic residues. The hydrolysis of the substrate (acetylcholine, ACh) is accomplished by the catalytic triad consisting of Ser200, Glu327, and His440, with Ser200 being transiently acetylated. Sussman et al. [2] have proposed a model for cation–π interactions [3] between the ammonium group of ACh and the aromatic amino acids (Tyr130, Trp84, and Phe330) of the active site. All these aromatic groups provide polarizable π electrons that might contribute to the induced, short-range, van der Waals interactions. The differential catalytic activity of Trp86Ala (Trp84 in *Tc*AChE) and Tyr337Ala (F330 in *Tc*AChE) human mutants [4] supports this hypothesis. It may also be noted that Trp84 is part of that Ω surface loop (Cys67–Cys94), which constitutes the thin portion of the long and narrow gorge, penetrating half-way into the enzyme and containing the catalytic site about 4 Å from its base [2].

The authors have examined, through combination of kinetic studies and molecular modeling, both the orientation of the Trp84 side chain and the conformational adjustment of the cysteine loop. This is the first time such an approach has been used to study these compounds (Figure 1, **3**–**7**).

## MATERIALS AND METHODS

All the reagents for synthesis of the inhibitors were purchased from Aldrich and were of analytical grade. AChE from *Electrophorus electricus* (Type V-S), acetylthiocholine (ATC), and 5,5-dithiobis(2-nitrobenzoic acid) (DTNB) were purchased from Sigma. Physovenine was provided by Prof. Arnold Brossi and Prof. Nigel H. Greig (NIH, Bethesda) [5] and 8-carbaphysostigmine was provided by Dr. Yuhpyng L.Chen (Pfizer, Groton, CT) [6]. The synthetic route to Phy analogs

*Correspondence to:* Dr. Massimo Pomponi.

Contract Grant Sponsor: Italian Ministero dell'Università e della Ricerca Scientifica e Tecnologica (MURST).

Contract Grant Sponsor: Consiglio Nazionale delle Ricerche (CNR).

(pyrrolo[2,3-b]indol-5-ol 3,3a,8,8a-hexahydro-1,3a,8-trimethyl-*N*-alkyl-carbamates, 3a*S-cis*) was similar in many respects to the one used for the synthesis of heptylphysostigmine [7].

### Preparation of Trimethyl-1,3a,8-hexahydro-1,2,3,3a,8,8a-pyrrol[2,3-b]indole-5(3a*S*, 8a*R*)-heptylphysostignine (6)

Five hundered and fifty milligrams of physostigmine (2 mmol) and 108 mg mmol of sodium methoxide (2 mmol) were placed in a flask (50 mL) to which a vacuum between 5 and 10 mm Hg was applied. Absolute ethanol (70 mL) was then added over 2 h in small volumes, under agitation at ambient temperature. When the ethanol had been removed, benzene (50 mL) was added (temperature range: ≈30°C). To this residue was slowly added 50 mL of a benzene solution containing 4 mmol of heptyl isocyanate; the reaction mixture was left to stand for 3 h, benzene being added when necessary. During this time, eseroline gets converted to carbamate. Benzene was evaporated, and petroleum ether was added to the reaction residue, followed by 10 mL of $10^{-3}$ M HCl. The vacuum was removed, and the crude reaction product was extracted with diethyl ether after previous saturation with sodium bicarbonate. The combined ether solutions were rapidly extracted with 50 mL of 0.05 M HCl. The aqueous acid solution, saturated with sodium bicarbonate, was again extracted with petroleum ether. The organic layer was repeatedly washed with water before being dried over sodium sulfate. The solvent was finally removed under vacuum. If necessary, the extract was chromatographed over a silica gel column, using chloroform/methanol (98:2) as eluent. The product was finally dissolved in benzene, heptane was added, and the solution was cooled. The residue slowly crystallized and had a m.p. of 83–86°C. UV spectrum in methanol: 303 (3300), 253 (14200). IR spectrum in chloroform: 3460 (m), 2920 (s), 2860 (s), 1720 (s), 1670 (s), 1600 (s), 1490 (s), 1240 (s), 1200 (s), 1120 (m). Structural assignment was confirmed by NMR spectroscopy on a $^1$H-(300 MHz) Varian Gemini spectrometer. NMR spectrum in deuterated benzene: 0.90 (t), 1.25 (s), 1.35 (s), 1.80 (t), 2.40 (s), 2.50 (t), 2.60 (s), 3.35 (q), 4.00 (s), 5.30–5.70 (m), 6.20 (d), 7.00 (s), 7.05 (dd). Mass spectrum (LKB Model 9000, single focusing): 359 (15), 218 (100), 174 (30), 161 (28), 160 (29).

### Preparation of Trimethyl-1,3a,8-hexahydro-1,2,3,3a,8,8a-pyrrol[2,3-b]indole-5(3a*S*,8a*R*)-decylphysostigmine (7)

The procedure for the preparation of **6** was followed. After evaporation of the solvent, an oily residue remained but was not crystallized. Inhibitors **7** and **6** presented similar UV and IR spectra. NMR spectrum in deuterated benzene: 0.90 (t), 1.25 (s), 1.40(s), 2.00 (t), 2.50 (s), 2.80 (t), 2.90 (s), 2.95–3.30 (m), 4.30 (s), 5.00–5.30 (m), 6.25 (dd), 6.65 (d), 6.75 (dd). Mass spectrum: 401 (13), 218 (100). Structures of the inhibitors used are shown in Figure 1.

### Enzyme Activity

AChE activities were measured in 0.1 M sodium phosphate buffer (pH 8) containing 0.1% BSA and 0.25 mM DTNB at 20°C according to Ellman et al. [8], using acetylthiocholine (ATC) as substrate. The reaction for fast-binding inhibitors was initiated by addition of substrate. When inhibition by the slow-binding inhibitors was measured, the reaction was started by the addition of enzyme. The assay medium contained 0.5 mM ATC iodide in a 0.1 M phosphate buffer (pH 7), and the reaction was monitored at 412 nm by means of a graphics software (Varian Cary 3E) at 20°C, using thermostated (Haake) cells. Typically, four inhibitor concentrations were used. The resulting dependence of activity on time was fit by nonlinear least-squares procedures [9] to the equation $v = (v_0 - v_{ss})e^{-kt} + v_{ss}$, where $v$ is the observed velocity at any time, $v_0$ is the initial velocity of the reaction, $v_{ss}$ is the steady-state velocity of the reaction, and $k$ is the pseudo-first-order rate constant. The equation applies whether the reaction is started by addition of the enzyme to the reaction

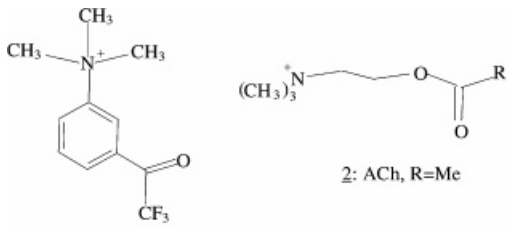


TMTFA, 1

2: ACh, R=Me

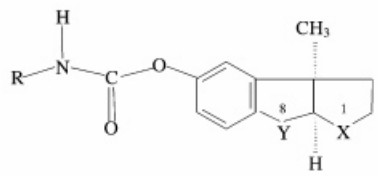


3-7

**FIGURE 1.** Molecular formulas: *m*-(*N*, *N*, *N*-trimethylammonio)-trifluoroacetophenone (TMTFA, **1**); ACh (**2**); 8-carbaphysostigmine (**3**, Y = $CH_2$, X = NEt, R = $CH_3$); physostigmine (Phy, **4**, Y = $NCH_3$, X = $NCH_3$, R = $CH_3$); physovenine (**5**, Y = $NCH_3$, X = O, R = $CH_3$); heptylphysostigmine (**Phy-C7**, **6**, Y = $NCH_3$, X = $NCH_3$, R = $C_7H_{15}$); decyl-Phy (**Phy-C10**, **7**, Y = $NCH_3$, X = $NCH_3$, R = $C_{10}H_{21}$).

mixture containing substrate and inhibitor or by the addition of substrate after preincubation of enzyme and inhibitor.

Building and analysis of the 3-D molecular models was performed on Silicon Graphics work stations, Indigo2 and O2, using the SYBYL modeling (in vacuo) software (TRIPOS, Inc. St. Louis, MO). The X-ray coordinates of *m*-(*N*,*N*,*N*-trimethylammonio)-trifluoroacetophenone–acetylcholinesterase (TMTFA–AChE) complex were used as templates. Specifically, the ligand was positioned to make a tetrahedral bond with the $O_\gamma$ of Ser200. Positioning of the ligand was also guided by interactions of quaternary nitrogen ($N^1$) with residue Trp84; the quaternary group was placed within van der Waals distance (~3.5 Å).

Initial optimization included restriction of the distances between the carbonyl oxygen of the amide nitrogen atoms of residues Gly118 and Gly119, which are two potential hydrogen bond donors. This restriction was relieved in the subsequent refinement. The POWELL minimizer was selected. The TRYPOS force field consisted of both van der Waals and electrostatic (Geisteiger–Marsili) energies. The cutoff criterion was 8 Å radius for all interactions. The energy convergence criterion was $\pm 0.1$ kcal mol$^{-1}$. The complexes have been superimposed using the $C_\alpha$ of α-helix 384–411 residues. This α-chain results the most invariant secondary structure for these intermediates.

## RESULTS

Physostigmine (**4**), caused reversible inhibition. The concentration value of the inhibitor in the assay was comparable to the inhibition constant, $K_i$ ($=k_{off}/k_{on}$), of the enzyme–inhibitor complex. These observations and the additional experiments are consistent with the following inhibition scheme (Scheme 1).

In the presence of inhibitor, the AChE activity dropped in a time-dependent manner that is well described by first-order kinetics. All the inhibitors produced complete inhibition of the enzyme. In accord with Scheme 1, the pseudo-first-order rate constant determined from the fit of the progress curve is described by the following equation [9]:

$$k_1 = (k_{on}/(1 + [S]/K_m))[\text{Inhibitor}] + k_{off} \qquad (1)$$

The Michaelis constant, $K_m$, was $0.11 \pm 0.01$ mM.

$$\text{E} + \text{Inhibitor} \underset{k_{off}}{\overset{k_{on}}{\rightleftharpoons}} \text{E-Inhibitor}$$

**SCHEME 1**

As predicted by this relation, the dependence of $k_1$ on inhibitor concentration was linear, from which $k_{on} = (3.5 \pm 0.2) \times 10^3$ M$^{-1}$ s$^1$ and $k_{off} = (1.7 \pm 0.4) \times 10^{-3}$ s$^{-1}$ (Figure 2A). The apparent association constant of the E–Inhibitor complex was $(2.0 \pm 0.5) \times 10^6$ M$^{-1}$. At high concentrations of **4** Eq. (1) reduced to $k_1 = (k_{on}/(1 + [S]/K_m))[\text{Inhibitor}]$. For inhibitor concentrations in the range 0.06–0.10 mM, the dependence of $k_1$ on **4** was linear (plot not shown). The value $k_{on} = (1.5 \pm 0.3) \times 10^3$ M$^{-1}$ s$^{-1}$ calculated from the slope of this plot was in good agreement with the value determined from Figure 2A. The same procedure was utilized for all the inhibitors used.

It is noteworthy, from the analysis of the numerical values of $k_{on}$ (Table 1) for charged and uncharged analogs, that charge does not confer a particular advantage for interaction in the active site. In order to verify the presence of any structural correlation, the tetrahedral intermediates generated during the inhibition step were structurally aligned on the crystallographic coordinates of the*Tc*AChE complex (Brookhaven Protein Data, ID Codes 1AMN) with the transition state analog inhibitor TMTFA [11], and then subjected to

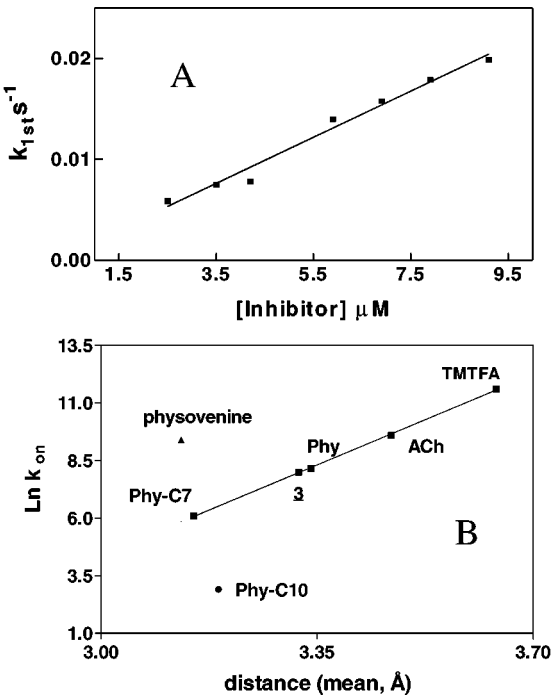


**FIGURE 2** (**A**) Dependence of the observed first-order inhibition rate constant on inhibitior concentration. The rate constants $k_{on}$ and $k_{off}$ were calculated from the slope (corrected for the presence of substrate) and intercept, respectively, of the displayed linear fit. Inhibition at 20°C. AChE activity was determined by a slight modification of the method used by Ellman et al. [8]. (**B**) Linear plot of $k_{on}$ vs the mean of the distances from indole ring of Trp84 (ligand–AChE complex). The plot allows us to derive the $k_{on}$ of ACh [10].

**TABLE 1.** Second-Order Rate Constant $k_{on}$ for Phy Analogs Inhibitors of Acetylcholinesterase

| *Inhibitor* | *ln* $k_{on}$ |
|---|---|
| TMTFA (**1**) | 11.6[a] |
| ACh (**2**) | 9.6[b] |
| **3** | 8.0 |
| **4** | 8.15 |
| **5** | 9.4 |
| **6** | 6.1 |
| **7** | 2.9 |

Enzyme inhibition was determined as described in Materials and Methods section. Values represent mean of triplicate determinations with standard deviation not exceeding 20%.

[a] Ref. [11].

[b] This value of $k_{on}$ ($\approx 1.4 \times 10^4$ $M^{-1}$ $s^{-1}$) is similar to the value of $k_{cat} \approx 1.4 \times 10^4$ $M^{-1}$ $s^{-1}$, reported by Rosenberry [10].

field-fit optimization. TMTFA, a potent inhibitor of AChE, forms a covalent complex with the enzyme that it structurally mimics the theoretical acylation tetrahedral intermediate [11,12] of acetylcholine (ACh). However, carbamates (for example, physostigmine) also react with AChE to produce a covalent, tetrahedral intermediate very similar to the complex formed during ACh hydrolysis. These analogies justify the similar approach that has been used in this study for TMTFA, Ach, and Phy analogs. In all cases the resultant complex corresponds to the tetrahedral geometry of an intermediate acylating/carbamoylating step of catalysis. The minimization has been successively performed using decreasing values of force constant from 100 to 0, kcal/((mole) $*$ (Å)$^2$; for this last value (without any constraint) the minimization has also been calculated in presence of charges. Notably, with or without constraints, there is no difference in the van der Waals distance of inhibitor from Trp84. Figure 3 shows the relative position of this residue for TMTFA (α-helix 384–411 was used for this superimposition).

In particular, the results, relative to the "cation–π interaction subsite" Trp84, were consistent with stacking of the positively charged ligand against the π electron system of residue at position 84, as suggested by the crystal structure [12]. In this context, Figure 4 shows the distances for the closer, positive atom of TMTFA. The mean of these distances ($3.64 \pm 0.01$ Å) correlate with the binding rate constant $k_{on}$. The same approach was also valid for ACh and physostigmine analogs. The most striking observation of the modeling study was a remarkable overall similarity between the orientation of the TMTFA molecule and the physostigmine analogs, i.e., the principal interactions appeared to be shared. In particular, the quaternary nitrogen ($N^1$ for physostigmine analogs) of the inhibitor was positioned within van der Waals distance (3.5 Å) of Trp84; the $O_\gamma$ of Ser200 lay within hydrogen-bonding distance of His440; Glu327 was also near His440. The oxygen (acceptor) of the inhibitor carbonyl group seemed to be stabilized in the tetrahedral intermediate by potential hydrogen bonds from the amide nitrogen of Gly118 and Gly119.

The relationship between the binding rate constant, $k_{on}$, and the mean of the relative distances (computed as reported in Figure 4) of indole rings of the side chain of Trp84 of each inhibitor-AChE complex is reported in Figure 2B. The result suggests a direct relationship between the relative distance from the Trp84 residue and the value of binding rate constant, $k_{on}$.

Phy (**4**) and 8-carbaphysostigmine (**3**) possess the amine group $N^1$, and at physiological pH, exist as cations. Since the indole nitrogen lone pair increases the electron density and partial negative charge of the aromatic system, the ammonium of an advancing ligand would induce electronic perturbations in the aromatic system, thus increasing the van der Waals interactions. At any rate, the catalytic machinery of AChE also seemed to utilize a second way of interaction typical of charged ligands. The coulombic effect of the positive ammonium group seemed to stabilize the tetrahedral intermediate and transition state with direct consequences on the value of $k_{on}$. If aromatic residues, particularly Trp84, are crucial for molecular recognition, the above observation may also apply to substrates.

The case is different for inhibitors **6** and **7**, where a specific steric effect seems to influence negatively the tetrahedral intermediate (Figure 3), which by a Hammond effect [13], produces a proportional destabilization of the transition state. In particular, compound **7**, which possesses the longer alkyl chain, caused a transient shift in the cysteine loop, Cys67–Cys94 (Figure 5). Apparently, this behavior was confined only to the presence of a significant steric effect.

An observation that can be added at this point is that the amine group ($N^1$) present in Phy (**4**) may not be essential for its anti-AChE activity. In fact, this was the noted in physostigmine analogs bearing oxygen at position 1 (physovenine, **5**). One reason for the activity of compound **5** may be that the aromatic electrons of indole ring of Trp84 modulate their charge density on the electronic environment of the ligand. However, a different contribution is also possible in this case as the $O^1$ oxygen can form a potential hydrogen bond with the hydroxy moiety of Tyr130.

## DISCUSSION

In this paper we compare the structure of TMTFA–*Tc*AChE complex [12] with those of selected inhibitor–*Tc*AChE complexes, with the goal of identifying particular topographical features that might be indicative of the inhibition mechanism. The results described herein

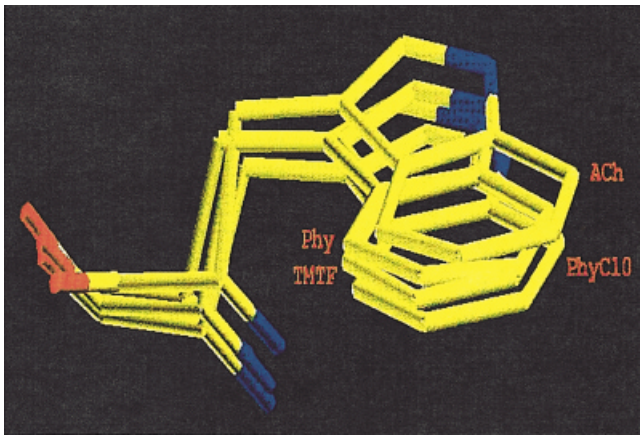


**FIGURE 3** Superimposition of TMTFA, ACh, Phy, and decyl-Phy (PhyC10) minimized structures showing the Trp84 shift. α-helix 384–411 has been used for this superimposition. The coordinates for TMTFA–AChE complex were obtained from Brookhaven Protein Data Bank (entry 1AMN). This molecular structure was used as the starting geometry for the minimization study. The carbamoyl (or carbonyl) group was positioned to make a tetrahedral bond with $O_\gamma$ of Ser200. The quaternary nitrogen of the inhibitor is positioned within van der Waals distance (3.5 Å); the $O_\gamma$ of Ser200 lies within hydrogen-bonding distance of His440; Glu327 is also near His440. No constraints were used. Procedure: ANNEAL (SYBYL): interesting region 18 Å; hot region 16 Å. TMTFA (**1**); ACh (**2**), RMS 0.36; Phy (**3**), RMS 0.25; decyl-Phy (PhyC10, **7**), RMS 0.22.

indicate that within a structural congeneric series (in this case analogs of the alkaloid Phy), in the inhibitor–AChE complex is observed a relationship between the bimolecular rate constant $k_{on}$ and the relative distances

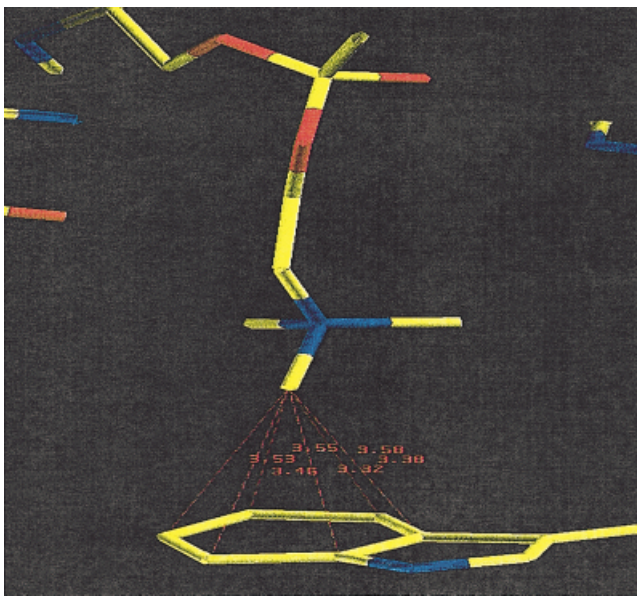


**FIGURE 4** 3-D structure of the "cation–π interaction subsite" Trp84 and inhibitor TMTFA, in the tetrahedral intermediate. The mean of the distances is considered to be proportional to the distance from the geometric center of the aromatic ring. Conditions as in Figure 3.

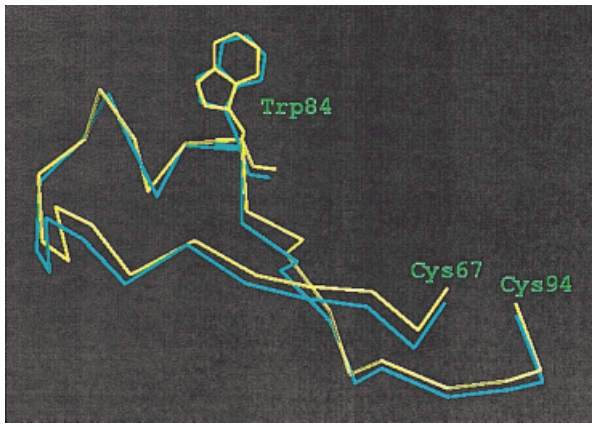


**FIGURE 5** Displacement of the Ω loop (Cys67–Cys94) structure in AChE. Superposition of the Ω loop trace of tetrahedral ACh complex and that of the modeled structure of decyl-Phy analog. Same conditions as for Figure 3. RMS 0.25. The Trp84 residue is linked to the helical turn structure (Ser79-Met83).

from the indolic ring of Trp84, computed as mean of these relative distances (Figures 4 and 2B).

However, the catalytic power of enzymes has long been attributed to specific interactions with substrates in the transition state. Since transition states have essentially zero lifetimes, it is impossible to observe them directly and information about their geometries must be acquired indirectly. The X-ray of the complex of *Tc*AChE with the transition state analog TMTFA is an example of how this data can be obtained. In addition, the manifest overall correspondence between the alignment of the TMTFA molecule and the physostigmine analogs provides a useful way of organizing inhibitors **3**–**6** (Figure 1) in the molecular modeling of tetrahedral intermediates. In addition, the results described herein (Figure 2B) show that charged and uncharged inhibitors follow a common correlation. This effect establishes that all compounds occupy a common site and share the principal interactions. The catalytic machinery of AChE also utilizes coulombic interactions, as suggested by data obtained for charged ligands. A consequence of this study is the feasibility extending this approach to substrates. In fact, the value of the ACh $k_{on}$ constant, calculated from the computational relative distance ($3.46 \pm 0.11$ Å), was $\approx 1.4 \times 10^4$ $M^{-1}$ $s^{-1}$ (vs. $1.4 \times 10^4$, reported by Rosenberry [10]).

According to this relationship the expected value $k_{on}$ for 8-carbaphysostigmine, $(2.9 \pm 0.2) \times 10^3$ $M^{-1}$ $s^{-1}$, is in a good agreement with the value reported in Table 1. Moreover, an additional comment is necessary for physovenine (**5**) and decyl-Phy (**7**). The $k_{on}$ value for physovenine may be due to the hard lone pairs of $O^1$, which generate a greater negative charge density while interacting with the partial negative charge of π system of indole ring of the Trp84 residue. On the other hand,

the behavior of decyl-Phy may be due to the unusual steric effect of the long alkyl chain. The refined and superimposed structures ACh (**2**) and decyl-Phy (**7**) reveal a conformational distortion of the cysteine loop (Cys67–Cys94) (Figure 5). From a structural point of view, other studies on AChE complexes with reversible inhibitors have shown very similar results [14].

The mobility of Trp84 and the dynamic behavior of the cysteine loop (Cys67–Cys94) bearing Trp84 has been a field of study that has provided very conflicting results [15,16]. In particular, molecular dynamics [15] suggests the existence of a molecular device (the shutter-like back door) that opens to admit or remove molecules, although site-directed mutagenesis studies failed to provide experimental support for the back door model [17]. In the present study, the adjustment of the loop was observed for the longer N-carbamyl chains (**7**). However, at the same time, the steric effects seemed to interfere with the validity of the present approach: when bulky inhibitors were squeezed into the binding pocket, the modeling showed that the cysteine loop moved away (Figure 5).

In conclusion, the authors hope that this procedure, and future studies based on steric effects, might help in discovering some features of the traffic of products from the active site of AChE. This traffic might be governed by the mobility of the cysteine loop and this dynamic behavior may be part of a more general mechanism of AChE catalysis.

## ACKNOWLEDGMENTS

The authors thank Professor Arnold Brossi and Prof. Nigel H. Greig (NIH, Bethesda), and Dr. Yuhpyng L. Chen (Pfizer, Groton, CT) for the kind gift of physovenine and 8-carbaphysostigmine, respectively.

## REFERENCES

1. (a) Taylor P. Development of acetylcholinesterase inhibitors in the therapy of Alzheimer's disease. Neurology 1998;51(1, Suppl 1):S30–S35, S65–S67; (b) Knopman DS. Current pharmacotherapies for Alzheimer's disease. Geriatrics 1998;53:S31–S34.
2. Sussman JL, Harel M, Frolow F, Oefner C, Goldman A, Toker L, Silman I. Atomic structure of acetylcholinesterase from Torpedo californica: A prototypic acetylcholine-binding protein. Science 1991;253:872–879. Entry PDB 2ACE; authors: Harel M, Raves ML, Silman I, & Sussman JL (23 June 1996).
3. Dougherty DA, Stauffer DA. Acetylcholine binding by a synthetic receptor: Implications for biological recognition. Science 1990;250:1558–1560.
4. Ordentlinch A, Barak D, Kronman C, Ariel N, Segall Y, Velan B, Shafferman A. Contribution of aromatic moieties of tyrosine 133 and of the anionic subsite tryptophan 86 to catalytic efficiency and allosteric modulation of acetylcholinesterase. J Biol Chem 1995;270(5):2082–2091.
5. Yu QS, Liu C, Brzostowska M, Chrisey L, Brossi A, Greig NH, Atack JR, Soncrant TT, Rapoport SI, Radunz HE. Physovenines: Efficient synthesis of (−)- and (+)-physovenine and synthesis of carbamate analogs of (−)-physovenine. Helv Chem Acta 1991;74:761–766.
6. Chen YL, Nielsen J, Hedberg K, Dunaiskis A, Jones S, Russo L, Ives J, Liston D. Syntheses, resolution, and structure-activity relationships of potent acetyl-cholinesterase inhibitors: 8-Carbaphysostigmine analogs. J Med Chem 1992;35:1429–1434.
7. Marta M, Gatta F, Pomponi M. Physostigmine analogs anticholin-esterases: Effects of the lengthening of the N-carbamic chain on the inhibition kinetics. Biochim Biophys Acta 1992;1120(3):262–266.
8. Ellman GL, Courtney KD, Andres V Jr, Featherstone M. A new and rapid colorimetric determination of acetylcholinesterase activity. Biochem Pharmac 1961;7: 88–95.
9. Williams JW, Morrison JF. The kinetics of reversible tight-binding inhibition. Methods Enzymol 1979;63:437–467.
10. (a) Rosenberry TL. Acetylcholinesterase. Adv Enzymol Relat Areas Mol Biol 1975;43:103–218; (b) Rosenberry TL, Barbett P, Mays C. Acetylcholinesterase. Methods Enzymol 1982;82(Pt A):325–339.
11. Nair HK, Seravalli J, Arbuckle T, Quinn DM. Molecular recognition in acetylcholinesterase catalysis: Free-energy correlations for substrates turnover and inhibition by trifluoro ketone transition-state analogs. Biochemistry 1994;33:8533–8576.
12. Harel M, Quinn DM, Nair HK, Silman I, Sussman JL. The X-ray structure of a transition state analog complex reveals the molecular origins of the catalytic power and substrate specificity of acetylcholinesterase. J Am Chem Soc 1996;118:2340–2346.
13. March J. The hammond postulate. In Advanced Organic Chemistry. London: McGraw-Hill; 1977. pp. 194–195.
14. Pomponi M, Marta M, Sacchi S, Colella A, Patamia M, Gatta F, Capone F, Oliverio A, Pavone F. Studies on a new series of THA analogs: Effects of the aromatic residues that line the gorge of AChE. FEBS Lett 1997;409(2):155–160.
15. Gilson MK, Straatsma TP, McCammon JA, Ripoll DR, Faerman CH, Axelsen PH, Silman I, Sussman JL. Open "back door" in a molecular dynamics simulation of acetylcholinesterase. Science 1994;263:1276–1278.
16. Kronman C, Ordentlich A, Barak D, Velan B, Shafferman A. The "back door" hypothesis for product clearance in acetylcholinesterase challenged by site-directed mutagenesis. J Biol Chem 1994;269(45):27819–27822.
17. Faerman C, Ripoll D, Bon S, Le Feuvre Y, Morel N, Massoulie J, Sussman JL, Silman I. Site-directed mutants designed to test back-door hypotheses of acetylcholinesterase function. FEBS Lett 1996;386(1):65–71.